INTERMEDIATES IN PHOTOCHEMISTRY OF Fe(III) COMPLEXES IN WATER

VICTOR PLYUSNIN, IVAN POZDNYAKOV, EUGENY GLEBOV, VJACHESLAV GRIVIN, NIKOLAI BAZHIN

Institute of Chemical Kinetics and Combustion SB RAS, Institutskaya 3, 630090 Novosibirsk, Russia, plyusnin@kinetics.nsc.ru

Abstract. The photochemistry of $Fe(OH)^{2+}$ complex and complexes formed by Fe(III) and pyruvic (Pyr), tartaric (Tart), sulfosalycilic (SSA) and oxalic (Ox) acids in aqueous solutions were studied by means of stationary and nanosecond laser flash photolysis. The application of different scavengers of transient radicals has shown that the hydroxyl radical is the primary photochemical species in photochemistry of the $FeOH^{2+}$ complex. In the photochemistry of $FePyr^{2+}$ and $FeTart^+$ complexes a weak absorption was found in the red spectral region which was attributed to $[Fe^{II}...R\text{-}COO^\bullet]^{2+}$ radical complexes. Laser flash photolysis of $FePyr^{2+}$ and $FeTart^+$ complexes in the presence of methyl viologen (effective scavenger of different free radicals) gave evidence of $MV^{\bullet+}$ radical cation formation with concentration as small as ~2% of Fe(III) complex disappeared. The reaction mechanism including inner-sphere electron transfer with the formation of $[Fe^{II}...R\text{-}COO^\bullet]^{2+}$ radical complex and its transformation to the reaction products is proposed. The main photochemical process for $Fe^{III}(C_2O_4)_3^{3-}$ complex in aqueous solutions was found to be intramolecular electron transfer from the ligand to Fe(III) ion with the formation of a primary radical complex $[(C_2O_4)_2Fe^{II}(C_2O_4^\bullet)]^{3-}$. The yield of free radical species (i.e., $CO_2^{\bullet-}$ and $C_2O_4^{\bullet-}$) was found to be less then 6% of $Fe^{III}(C_2O_4)_3^{3-}$ disappeared after a laser pulse.

Keywords: photochemical process, Fe (III) complexes, organic acid ligands, laser flash photolysis.

1. Introduction

The most photochemically active spectral region of solar irradiation near 300 nm (290–310 nm) gives $\geq 10^{-2}$ M quanta per year [1] in layer about 10 m of ocean or river waters. This value exceeds the concentration of many impurities in natural waters (10^{-4}–10^{-6} M), and the photochemical reactions can play an important role

in their transformation. Iron is the most abundant transition metal, typically found in concentrations of several µM in natural waters. Carboxylic acids are considered to be one of the dominant classes of organic compounds found in natural waters. Therefore, the photochemistry of iron hydroxo- and carboxylic complexes has received considerable attention over the past 50 years.

The literature [2] mechanism of Fe(III) hydroxocomplexes photolysis in water solutions is based on intramolecular electron transfer from the coordinated OH^- anion to the central ion of the excited complex with subsequent escape of a hydroxyl radical into the bulk. It is assumed that the oxidation of organic compounds is initiated by the $^{\bullet}OH$ radical. This mechanism was, however, usually based on the results of analysis of only final products of phototransformations. $^{\bullet}OH$ radical in water solutions has a weak absorption in the far UV spectrum region (a band with a maximum at 225 nm and absorption coefficient of about 500 M^{-1} cm^{-1} [3]) not easily accessible for recording because of the absorption of initial complexes. Therefore, in time-resolved photochemical experiments it can be revealed using a trap, i.e., a molecule that, in reactions with OH radical, forms an intermediate with a characteristic absorption spectrum.

The presence of carboxylic acids, in the forms of oxalate, citrate ions and so on, has a significant effect on photoactivity of Fe(III) ions, because they may form stable complexes with Fe(III) ions. The primary photochemical process for Fe(III) complexes with carboxylic acids was proposed to be an inner-sphere electron transfer with the formation of Fe(II) complex and an escape of an organic radical to the solvent bulk followed by its decarboxylation [4]. The secondary radical formed as the result of decarboxylation could react with the different components of the reaction system (e.g., Fe(III) complexes or molecular oxygen). Reaction mechanisms put forward on the basis of the nature and content of the final reaction products should be verified by the experiments on the observation of the proposed intermediates.

The aim this work was to observe intermediates in the photochemistry of $FeOH^{2+}$ complex and Fe(III) carboxylic complexes with sulfosalycilic (FeSSA), pyruvic ($FePyr^{2+}$), tartaric ($FeTart^+$) and oxalate ($FeOx_3^{3-}$) ions (structures of these complexes are shown in Fig. 1.1).

For recording of the intermediates, which have no absorption in the suitable spectral region, one needs to use scavengers. A scavenger should react with the studied intermediate to form another short-living species, which has a characteristic and intensive absorption in a suitable spectral region. In case of photochemistry of $FeOH^{2+}$ complex N,N-dimethylformamide (DMFA), benzene, phenol (PhOH) and nitrobenzene ($PhNO_2$) as the $^{\bullet}OH$ radical scavengers were used. In some other cases the dication of methyl viologene (MV^{2+}) was used as the scavenger of primary transient radicals. The molar absorption coefficient for the $MV^{\bullet+}$ radical cation in water is equal to 41,500 M^{-1} cm^{-1} at 396 nm [5].

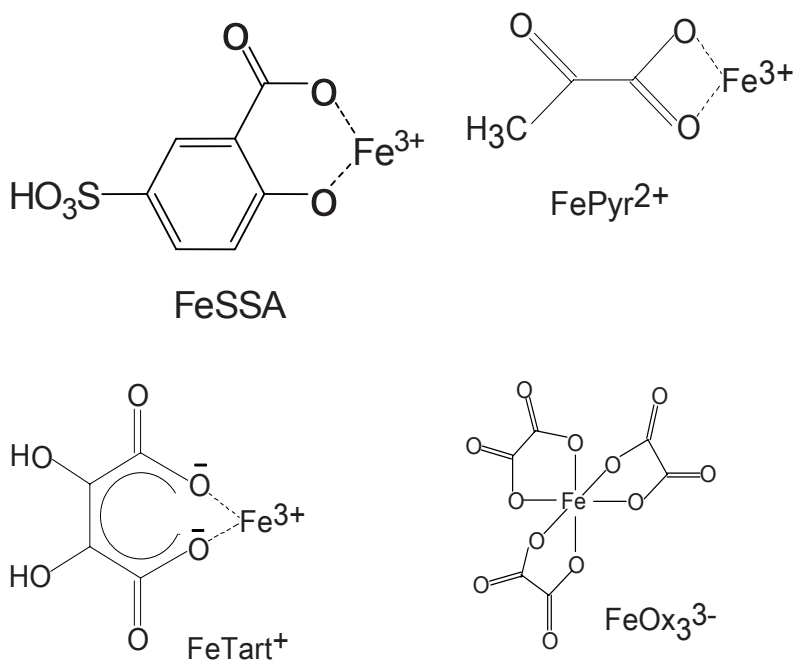**Fig. 1.** Structures of Fe(III) carboxylic complexes with sulfosalycilic (FeSSA), pyruvic (FePyr^{2+}), tartaric (FeTart$^+$) and oxalate (FeOx$_3^{3-}$) ions.

2. Experimental

A set-up for laser flash photolysis with XeCl (308 nm, 15 ns, 30 mJ) or YAG:Nd (355 nm, 7 ns, 40 mJ/pulse) laser excitation [6] was used in the experiments. A steady-state photolysis was performed using irradiation of either a XeCl and YAG:Nd lasers or a high-pressure mercury lamp with a set of glass filters for the separating the necessary wavelengths. Electron absorption spectra were recorded using HP 8354 spectrophotometers. The analysis of the final products of photo-chemical reactions was performed by HPLC (SP8800-20 "Spectra Physics" chromatograph with an UV detector). For the numerical calculations of the kinetic curves of flash photolysis, the differential equations were solved by means of the fourth-order Runge-Kutta method.

As a source of Fe(III) ions, Fe(ClO$_4$)$_3$ × H$_2$O (Aldrich) was used. The absorption spectrum of Fe(OH)$^{2+}$ complex contains charge transfer bands with maxima at 208 and 300 nm (absorption coefficients at these wavelengths are 4,300 and 1,985 M^{-1} cm^{-1}, respectively [2]). All the experiments with FeOH^{2+} complex were

carried out in solutions with pH ≈ 3. In these conditions, the ions of trivalent iron form the complexes $Fe(OH)^{2+}$ (90 %) and $Fe^{3+}(aq)$ (10 %) [2]. Since the absorption coefficient of hydroxo-complex at the wavelength of laser radiation (308 or 355 nm) is much higher than that of $Fe^{3+}(aq)$, the only photoactive form in the experiments was the $FeOH^{2+}$ complex.

The concentration of scavengers was much higher than that of the other substances, such as Fe(III) or ligands and was enough to capture all of transient radicals generated in the photoreaction. In spite of low absorption at 308 and 355 nm, a scavenger does not display any photochemical activity under excitation at these wavelengths, which is necessary for its application as a trap of transient radicals. All experiments were performed in oxygen-free samples with double-distilled water. When preparing samples with $Fe(OH)^{2+}$ complex, the water was also additionally treated by irradiating Fe(III) perchlorate solution for several hours with the light of a high-pressure mercury lamp to remove the organic impurities.

3. Results and discussion

3.1. The •OH radical formation in photochemistry of $FeOH^{2+}$ complex [7–11]

Experiments on the laser flash photolysis of $Fe(OH)_{aq}^{2+}$ in presence of organic additives (nitrobenzene 10^{-5}–10^{-4} M, DMFA 10^{-5}–10^{-2} M and phenol 10^{-5}–10^{-4} M) have demonstrated the formation of an intermediate absorption. A characteristic time of an increase of the signals reduces with the enhancing the concentration of organic traps of •OH radical. The intermediate absorption spectra have maxima at 410 and 380 nm in presence of nitrobenzene and DMFA and correspond to the $Ph(•OH)NO_2$ [12] and $HCON(CH_2•)(CH_3)$ [13] radicals. In presence of phenol, the initial intermediate absorption spectrum has a maximum at 335 nm corresponding to that of the radical $Ph(OH)_2•$ [14]. After formation, the spectrum of $Ph(OH)_2•$ is transformed to the new absorption bands with maxima at 380 and 400 nm. These data coincide with those obtained in [14] (pulse radiolysis of aqueous phenol solutions). It is shown in [28], that the $Ph(OH)_2•$ radical eliminates a molecule of water with the formation of phenoxyl $(PhO•)$ radical. $PhO•$ radical has two narrow close-located absorption bands at 380 and 400 nm and rather poorly absorbs in the region of $\lambda < 350$ nm [14, 15]. The observation of the kinetic curves of the formation of organic radicals for all the systems clearly supports the occurrence of these species in the reactions between •OH radical and organic traps.

The •OH radical can be added to a nitrobenzene molecule in three different positions to form three isomers. However, the data on the difference between the optical spectra of isomers are unavailable in the literature. Therefore, their spectra

are assumed to coincide. The proposed mechanism of reactions is described by kinetic scheme (1–5) in which the primary reaction (1) is responsible for hydroxyl radical formation:

$$Fe(OH)^{2+} \xrightarrow{\ h\nu\ } Fe^{2+}(aq) + {}^{\bullet}OH \qquad \varphi = 0.2 \tag{1}$$

$${}^{\bullet}OH + PhNO_2 \longrightarrow Ph({}^{\bullet}OH)NO_2 \qquad k_2 = 4.7 \times 10^9\,M^{-1}\,s^{-1} \tag{2}$$

$$2\,{}^{\bullet}OH \longrightarrow H_2O_2 \qquad 2k_3 = 5.2 \times 10^9\,M^{-1}\,s^{-1} \tag{3}$$

$$2\,Ph({}^{\bullet}OH)NO_2 \longrightarrow products \qquad 2k_4 = 2.7 \times 10^9\,M^{-1}\,s^{-1} \tag{4}$$

$${}^{\bullet}OH + Fe^{2+}(aq) \longrightarrow Fe(OH)^{2+} \qquad k_5 = 4.7 \times 10^9\,M^{-1}\,s^{-1} \tag{5}$$

The results of modeling the experimental curves with different concentrations of nitrobenzene and $Ph({}^{\bullet}OH)NO_2$ radicals (varied by change in laser pulse intensity) allow to get the rate constants of all reactions in scheme (1–5). The absorption coefficient of the band at 410 nm of $Ph({}^{\bullet}OH)NO_2$ radical was calculated as $\varepsilon = 5660\,M^{-1}\,cm^{-1}$.

3.2. Possible processes of ${}^{\bullet}OH$ radical formation upon the excitation of $FeOH^{2+}$ complex [8]

One can suggest the different mechanisms of ${}^{\bullet}OH$ radical formation in reactions involving the light-excited $[FeOH^{2+}]^*$ complex:

M1. The intrasphere electron transfer from hydroxide ion with subsequent escape of ${}^{\bullet}OH$ radical into the bulk

$$[FeOH^{2+}]^* \longrightarrow [Fe^{2+}({}^{\bullet}OH)] \tag{6}$$

$$[Fe^{2+}({}^{\bullet}OH)] + H_2O \longrightarrow Fe^{2+}(aq) + {}^{\bullet}OH \tag{7}$$

M2. Electron transfer from the second coordination sphere accompanied by proton transfer into the solvent bulk

$$Fe(OH)^{2+} + H_2O \longrightarrow Fe^{2+}(OH^-) + {}^{\bullet}OH + H^+ \tag{8}$$
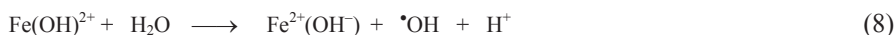
M3. Hydrogen atom transfer from the second to the first coordination sphere

$$Fe(OH)^{2+} + H_2O \longrightarrow Fe^{2+}(aq) + {}^{\bullet}OH \tag{9}$$

It was tried to determine the mechanism of hydroxyl radical formation based on the temperature dependence of quantum yield. The idea is that when realizing mechanisms M2 and M3, based on tunneling, the activation energy of quantum yield should tend to zero. Process M1 includes the reaction of exchange of a hydroxyl radical to a water molecule in the first coordination sphere of Fe^{2+} ion.
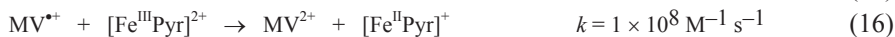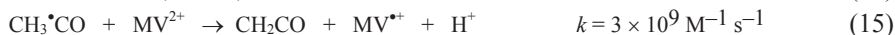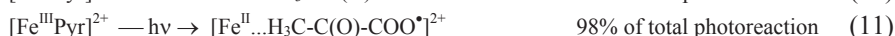
It should possess considerable activation energy typical of the reactions of photo-aquation (for $FeOH^{2+}$ ion the activation energy of water molecule exchange in the first coordination sphere is 34.7 kJ mol^{-1} [16]). Thus, in the case of great activation energy of quantum yield, one could suggest, with great probability, the realization of mechanism (M1).

The method of laser flash photolysis was used to measure the quantum yield of hydroxyl radical upon photolysis of $FeOH^{2+}$ complex in the presence of nitrobenzene. The absolute value of $^{\bullet}OH$ radical quantum yield at 298 K was found to be 0.2, which is in fair agreement with the value of 0.195 obtained upon excitation at 310 nm [2]. However, the activation energy is only 10.0 ± 1.3 kJ mol^{-1} and this low value does not allow one to choose among the different photolysis mechanisms M1, M2, and M3.

3.3. Photochemistry of Fe(III)-Pyr complex

The UV spectrum of $FePyr^{2+}$ complex was reported previously [17]. It exhibits a charge transfer band with maximum at 323 nm ($\varepsilon = 1550$ M^{-1} cm^{-1}) and more intense bands at shorter wavelengths. The stability constant (pK = 4.83) of $[Fe^{III}Pyr]^{2+}$ was calculated in [18]. Taking into account the dissociation constant of pyruvic acid (pKa = 2.5 [19]) and the equilibrium constants for Fe(III) hydroxo-complex [20]), the content of $[Fe^{III}Pyr]^{2+}$ complex for total concentrations of Fe(III) and pyruvate anion 5×10^{-4} M and 1.5×10^{-3} M, correspondingly, at pH 3 was about 86%. The quantum yield of $[Fe^{III}Pyr]^{2+}$ photolysis for deaerated solutions was found to be 1.0 ± 0.1.

In the experiments on laser flash photolysis a weak absorption was found in the spectral region of 580–720 nm. This absorption was attributed to $[Fe^{II}...H_3C-C(O)-COO^{\bullet}]^{2+}$ radical complex. Laser flash photolysis of $[Fe(Pyr)]^{2+}$ in the presence of methyl viologen (MV^{2+} dication) gave evidence of $MV^{\bullet+}$ radical cation formation. Its initial concentration was found to be as small as 2% of $[Fe(Pyr)]^{2+}$ disappeared. The reaction mechanism including inner-sphere electron transfer with the formation of $[Fe^{II}...H_3C-C(O)-COO^{\bullet}]^{2+}$ radical complex and its transformation to the reaction products is proposed.

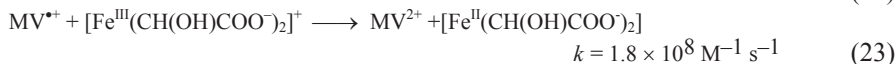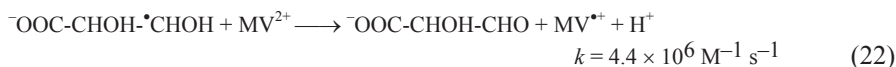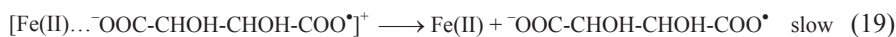|		
$[Fe^{III}Pyr]^{2+} \xrightarrow{hv} Fe^{2+} + H_3C-C(O)-COO^{\bullet}$	2% of total photoreaction	(10)
$[Fe^{III}Pyr]^{2+} \xrightarrow{hv} [Fe^{II}...H_3C-C(O)-COO^{\bullet}]^{2+}$	98% of total photoreaction	(11)
$[Fe^{II}...H_3C-C(O)-COO^{\bullet}]^{2+} \longrightarrow Fe^{2+} + H_3C-C(O)-COO^{\bullet}$	slow	(12)
$H_3C-C(O)-COO^{\bullet} \rightarrow CH_3^{\bullet}CO + CO_2$	fast (0.01-1 µs)	(13)
$2\,CH_3^{\bullet}CO \rightarrow (CH_3CO)_2$	$2k = 2 \times 10^9$ M^{-1} s^{-1}	(14)
$CH_3^{\bullet}CO + MV^{2+} \rightarrow CH_2CO + MV^{\bullet+} + H^+$	$k = 3 \times 10^9$ M^{-1} s^{-1}	(15)
$MV^{\bullet+} + [Fe^{III}Pyr]^{2+} \rightarrow MV^{2+} + [Fe^{II}Pyr]^+$	$k = 1 \times 10^8$ M^{-1} s^{-1}	(16)

So, the major channel of the $[Fe^{III}Pyr]^{2+}$ photoreaction seems to be the formation of the transient $[Fe^{II}...H_3C\text{-}C(O)\text{-}COO^\bullet]^{2+}$ radical complex. The formation of a weak absorption band in the region of 650 nm is a manifestation of the radical complex. The decay of the radical complex leads to the reaction products.

3.4. *Photochemistry of Fe(III)-Tart complex* [21]

The UV spectrum of Fe(III)-Tart complex contains a charge transfer band with maximum at 345 nm ($\varepsilon = 1600$ M^{-1} cm^{-1}) and more intense bands at shorter wavelengths. $[Fe^{III}Tart]^+$ complex was prepared from iron(III) perchlorate (Aldrich) and tartaric acid (Aldrich). The typical concentrations of the both reagents were 5×10^{-4} M at pH 3.0. It is evident from the equilibrium constants (lg $K_1 = 7.49$ and lg $K_2 = 11.86$ [22]) that ca. 86% of Fe(III) was forming the $[Fe^{III}Tart]^+$ complex. The goal of the study was the search of suitable and effective scavenger for short-living intermediates formed upon the photolysis of $[Fe^{III}Tart]^+$ complex. To solve the problem, methyl viologen dication (MV^{2+}) was used as a scavenger for the organic radicals.

The photolysis of $[Fe^{III}Tart]^+$ in the absence of MV^{2+} leads only to the instant bleaching in the region of the absorption band of the initial complex. It means that the absorption of the intermediates in the region of 300–800 nm, if exists, is weak. If MV^{2+} is added, the instant decrease in absorption due to the disappearance of $[Fe^{III}Tart]^+$ is superimposed with the formation of new sharp bands of $MV^{\bullet+}$ radical cation in the region of 370–400 nm and a less intensive band with the maximum at 605 nm [5]. $MV^{\bullet+}$ radical cation is formed in the reaction of MV^{2+} with an organic $^-COOH\text{-}CHOH\text{-}{}^\bullet CHOH$ radical anion, which is the product of decarboxylation of the primary radical anion $^-COOH\text{-}CHOH\text{-}CHOH\text{-}COO^\bullet$. The rate of $MV^{\bullet+}$ decay was found to increase with the concentration of the initial complex. It means that the radical anion disappears in the reaction with $[Fe^{III}Tart]^+$. This mechanism is analogous to the case of photolysis of Fe(III)-Pyr.

$[Fe^{III}Tart]^+ \;\;—\, h\nu \rightarrow Fe(II) + {}^-OOC\text{-}CHOH\text{-}CHOH\text{-}COO^\bullet$ (17)

$[Fe^{III}Tart]^+ \;\;—\, h\nu \rightarrow [Fe(II)...{}^-OOC\text{-}CHOH\text{-}CHOH\text{-}COO^\bullet]^+$ (18)

$[Fe(II)...{}^-OOC\text{-}CHOH\text{-}CHOH\text{-}COO^\bullet]^+ \longrightarrow Fe(II) + {}^-OOC\text{-}CHOH\text{-}CHOH\text{-}COO^\bullet$ slow (19)

$^-OOC\text{-}CHOH\text{-}CHOH\text{-}COO^\bullet \longrightarrow {}^-OOC\text{-}CHOH\text{-}{}^\bullet CHOH + CO_2$ fast (20)

$2\,{}^-OOC\text{-}CHOH\text{-}{}^\bullet CHOH \longrightarrow$ products $2k = 6 \times 10^8$ M^{-1} s^{-1} (21)

$^-OOC\text{-}CHOH\text{-}{}^\bullet CHOH + MV^{2+} \longrightarrow {}^-OOC\text{-}CHOH\text{-}CHO + MV^{\bullet+} + H^+$

                                         $k = 4.4 \times 10^6$ M^{-1} s^{-1} (22)

$MV^{\bullet+} + [Fe^{III}(CH(OH)COO^-)_2]^+ \longrightarrow MV^{2+} + [Fe^{II}(CH(OH)COO^-)_2]$

                                         $k = 1.8 \times 10^8$ M^{-1} s^{-1} (23)

Literature does not contain information on the decarboxylation rate constants for the radical anions like $^-$OOC-CHOH-CHOH-COO$^•$, which have no absorption in the spectral range convenient for recording. It might be worth to note that the rate constants of decarboxylation were measured for different aryloxyl radicals, which have an intensive absorption in the visible spectral region. These rate constants are in the range of $10^6 - 5 \times 10^7$ s^{-1} [23].
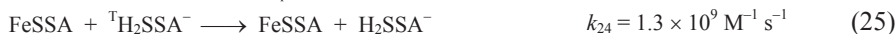
3.5. *Photochemistry of FeSSA complex [24, 25]*

The spectrum of FeSSA complex contains a charge transfer band with maximum at 505 nm ($\varepsilon = 1800$ M^{-1} cm^{-1}) [26]. In the UV region, FeSSA complex displays a stronger band with $\lambda_{max} = 286$ nm. The absorption band with a maximum at 297 nm is typical of the free non-coordinated SSA ligand. Concentrations of Fe(III) ions and SSA were usually about 10^{-4} M and 3×10^{-4} M, accordingly. All experiments were carried out with oxygen-free samples at pH = 3 and 298 K. The experiments on pump-probe femtosecond spectroscopy were described in [25].

Just after excitation of the complex with a femtosecond pulse ($\lambda_{ex} = 530$ nm), a bleach of the 505 nm absorption band was observed. The absorption of the complex is almost completely recovered after about 5 ps, which is in fair agreement with a photochemical stability of the complex under steady state irradiation in the visible region. The analysis of this time profile by iterative reconvolution of a biexponential function with the instrument response function gives the time constants $\tau_1 = 260$ fs and $\tau_2 = 1.8$ ps. Such biphasic dynamics is rather typical for ultrafast ground state recovery upon CT excitation [27]. Excitation in the CT band is followed by an ultrafast internal conversion to the vibrationally hot electronic ground state, which is then thermalized by vibrational cooling. Therefore, the 260 fs component is ascribed to the internal conversion while the 1.8 ps is assigned to the vibrational cooling.

Although FeSSA complex itself does not exhibit any photochemical activity, stationary irradiation (excimer XeCl laser, $\lambda_{ex} = 308$ nm) of solutions containing both complex and free ligand initiates a rather effective disappearance of the FeSSA complex absorption. The flash excitation ($\lambda_{ex} = 308$ nm) is followed by the buildup of the absorption band with a maximum at 440 nm. A study of the spectroscopy and photochemistry of SSA aqueous solutions indicates that this band is due to the absorption of excited triplet state of free ligand ($^TH_2SSA^-$) [24], which results from the absorption of light by the free, non-coordinated HSSA^{2-}. When HSSA^{2-} is excited into the singlet S$_1$ state (308 nm), the triplet state of $^THSSA^{2-}$, which has a T-T absorption band with a maximum at 470 nm, is populated with a quantum yield of $\varphi_T = 0.34$ [24]. In acidic solution (pH = 3), the $^THSSA^{2-}$ is rapidly protonated to form the $^TH_2SSA^-$, whose band shifts to 440 nm and has an absorption coefficient of 6.2×10^3 M^{-1} cm^{-1} [24].

The absorption of $^TH_2SSA^-$ decays within about 20 μs with a simultaneous buildup of a broad bleaching band (negative optical density) at 505 nm caused by the decreased FeSSA absorption. After the disappearance of $^TH_2SSA^-$ (50 μs), the spectrum still contains an absorption band at 400 nm, which belongs to the $HSSA^{2-•}$ radical [24]. Thus, the quenching of $^TH_2SSA^-$ can occur by both electron transfer (24) leading to FeSSA reduction and energy transfer (25). In the latter case, the physical quenching causes no changes in the oxidation state of the Fe(III) ion.

$$FeSSA + {}^TH_2SSA^- \longrightarrow Fe_{aq}^{2+} + HSSA^{•} + HSSA^{2-} \qquad k_{24} = 9 \times 10^8 \ M^{-1} \ s^{-1} \qquad (24)$$

$$FeSSA + {}^TH_2SSA^- \longrightarrow FeSSA + H_2SSA^- \qquad k_{24} = 1.3 \times 10^9 \ M^{-1} \ s^{-1} \qquad (25)$$

Thus, when the solution contains both FeSSA and non-coordinated $HSSA^{2-}$ ligand, UV irradiation causes a photo-reduction of the complex. This process is due to the electron transfer from the non-coordinated ligand in the triplet state to the FeSSA complex. The energy transfer between these species, which fails to cause any photochemical reaction, competes with the electron transfer. As applied to photo-processes in natural water, the data obtained allow us to define one of the important mechanisms of photo-degradation of organic compounds in anaerobic conditions, i.e., the photo-reduction of transition metal complexes due to the electron transfer from the long-lived triplet states of organic aromatic acids.

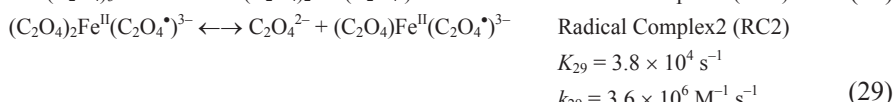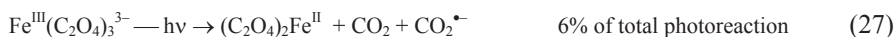## 3.6. *Photochemistry of Fe(III)-oxalate complex [28]*

Among Fe(III)-(poly)carboxylate complexes the photochemistry of trioxalate Fe(III) complex $(Fe^{III}(C_2O_4)_3{}^{3-})$ is of intense interest because this species exhibits high photochemical activity in natural waters under sunlight [29] and is widely used as stable and sensitive chemical actinometer [30]. The total process of $Fe^{III}(C_2O_4)_3{}^{3-}$ photolysis could be presented by reaction (26) [31]

$$2 \ Fe^{III}(C_2O_4)_3{}^{3-} \xrightarrow{\text{hv}} 2 \ Fe^{II}(C_2O_4{}^{2-})_2{}^{2-} + 2CO_2 + C_2O_4{}^{2-} \qquad (26)$$

The quantum yield of Fe(II) formation in reaction (26) is independent on the excitation wavelength in the range 270–365 nm and equals to 1.24 [30]. There are two different points of view on the primary photo-process following by excitation of $Fe^{III}(C_2O_4)_3{}^{3-}$. One of them is intramolecular electron transfer from the ligand to Fe(III) ion. The long-lived excited state, the radical complex $[(C_2O_4)_2Fe^{II}(C_2O_4{}^{•})]^{3-}$ or the $C_2O_4{}^{•-}$ radical are proposed as primary intermediate(s) [32, 33]. Another mechanism is the sequential cleavage of Fe(III)-O bond (between one oxalate ligand and Fe(III) ion) and the C-C bond of the ligand. Biradical complex $[(C_2O_4)_2Fe^{III}(CO_2{}^{•})_2]^{3-}$ [34] or $CO_2{}^{•-}$ radical are assumed as primary intermediate(s) [35, 36].
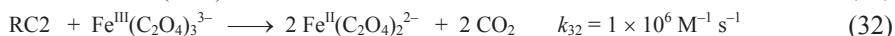
Laser flash photolysis experiments carried out in the wide range of initial parameters provide new evidences that intramolecular electron transfer from ligand to Fe(III) ion is a main photochemical process in $Fe^{III}(C_2O_4)_3^{3-}$ photochemistry. As primary intermediate the radical complex $(C_2O_4)_2Fe^{II}(C_2O_4^{\bullet})^{3-}$ is formed, yield of organic radicals in the primary photo-process is negligible.

Kinetic scheme of $Fe^{III}(C_2O_4)_3^{3-}$ photolysis was proposed including formation of $(C_2O_4)_2Fe^{II}(C_2O_4^{\bullet})^{3-}$ (in ground electronic state), its reversible dissociation on the oxalate ion and secondary radical complex $(C_2O_4)Fe^{II}(C_2O_4^{\bullet})^{-}$ and decay of both radical complexes. In the framework of this scheme absorption spectra and rate constant of formation and decay of all intermediates were determined.

$Fe^{III}(C_2O_4)_3^{3-} - h\nu \rightarrow (C_2O_4)_2Fe^{II} + CO_2 + CO_2^{\bullet-}$	6% of total photoreaction	(27)
$Fe^{III}(C_2O_4)_3^{3-} - h\nu \rightarrow (C_2O_4)_2Fe^{II}(C_2O_4^{\bullet})^{3-}$	Radical Complex1 (RC1)	(28)
$(C_2O_4)_2Fe^{II}(C_2O_4^{\bullet})^{3-} \longleftrightarrow C_2O_4^{2-} + (C_2O_4)Fe^{II}(C_2O_4^{\bullet})^{3-}$	Radical Complex2 (RC2)	
	$K_{29} = 3.8 \times 10^4 \text{ s}^{-1}$	
	$k_{29} = 3.6 \times 10^6 \text{ M}^{-1} \text{ s}^{-1}$	(29)
$RC1 \longrightarrow Fe^{II}(C_2O_4)_2^{2-} + C_2O_4^{\bullet-}$	$k_{30} = 1.5 \times 10^2 \text{ s}^{-1}$	(30)
$RC2 \longrightarrow Fe^{II}(C_2O_4) + C_2O_4^{\bullet-}$	$k_{31} = 2.0 \times 10^2 \text{ s}^{-1}$	(31)
$RC2 + Fe^{III}(C_2O_4)_3^{3-} \longrightarrow 2 Fe^{II}(C_2O_4)_2^{2-} + 2 CO_2$	$k_{32} = 1 \times 10^6 \text{ M}^{-1} \text{ s}^{-1}$	(32)

The addition of MV^{2+} to the solutions containing $Fe^{III}(C_2O_4)_3^{3-}$ leads to formation and decay of additional transient absorption signal at 396 nm of the $MV^{\bullet+}$ radical cation. The observed rate constant of the signal formation depends linearly on MV^{2+} concentration. The bimolecular rate constant of $MV^{\bullet+}$ formation $k \approx 1.2 \times 10^{10} \text{ M}^{-1} \text{ s}^{-1}$ is close to value of the rate constant of reaction of $CO_2^{\bullet-}$ radical with MV^{2+} [24]. However, the yield of $MV^{\bullet+}$ radical cation (and $CO_2^{\bullet-}$ radical, respectively) is lower than 6% of total $Fe^{III}(C_2O_4)_3^{3-}$ photo-decay. So, the main way of photoreaction is the $(C_2O_4)_2Fe^{II}(C_2O_4^{\bullet})^{3-}$ radical complex (RC1) formation.

4. Conclusions

Mechanisms of primary photochemical processes are revised for several Fe(III) complexes with organic acids ligands. Intramolecular electron transfer from ligand to Fe(III) ion with the formation of transient radical complex is the main photochemical process for Fe(III) complexes with carboxylic acids. Spectral and kinetic parameters of transient species, such as free radicals and radical complexes, are determined.

References

1. http://science.nasa.gov/headlines/images/sunbathing/sunspectrum.htm.
2. Benkenberg H-J, Warneck P (1995) *J Phys Chem*, 99: 5214.
3. Buxton GV, Greenstock CL, Helman WP, Ross AB (1988) *J Phys Chem Ref Data*, 17: 513.
4. Nansheng D, Feng W, Fan L, Mei X (1998) *Chemosphere*, 36: 3101.
5. Watanabe T, Honda K (1982) *J Phys Chem,* 86: 179.
6. Grivin VP, Khmelinski IV, Plyusnin VF, Blinov II, Balashev KP (1990) *J Photochem Photobiol A:Chem*, 51: 167.
7. Ivanov KL, Glebov EM, Plyusnin VF, Ivanov YuV, Grivin VP, Bazhin NM (1999) *React Kinet Catal Lett*, 66: 163.
8. Pozdnyakov IP, Glebov EM, Plyusnin VF, Grivin VP, Ivanov YuV, Vorobyev DYu, Bazhin NM (2000) *Pure Appl Chem*, 72: 2187.
9. Pozdnyakov IV, Glebov EM, Plyusnin VF, Grivin VP, Ivanov YuV, Bazhin NM, Vorobjev DYu (2000) *Mendeleev Commun*, 10: 185.
10. Pozdnyakov IP, Sosedova YuA, Plyusnin VF, Glebov EM, Grivin VP, Vorobyev DYu, Bazhin NM (2004) *Int J Photoenergy*, 6: 89.
11. Pozdnyakov IP, Sosedova YuA, Plyusnin VF, Grivin VP, Vorobyev DYu, Bazhin NM (2004) *Russian Chem Bull*, International Edition, 53: 2715.
12. Asmus K-D, Cercek B, Evert M, Henglein A (1967) *Wigger A Trans Faraday Soc*, 63: 2435.
13. Hayon E, Ibata T, Lichtin NN, Simic M (1970) *J Am Chem Soc*, 92: 3898.
14. Land EJ, Ebert M (1967) *Trans Far Soc*, 63: 1181.
15. Field RJ, Raghavan NV, Drummer JG (1982) *J Phys Chem*, 86: 2443.
16. Swift TJ, Connick RE (1962) *J Chem Phys*, 37: 307.
17. Wang L, Zhang Ch, Wu F, Deng N, Glebov EM, Bazhin NM (2006) *React Kinet Catal Lett*, 89: 183.
18. Ghandour M, Mansour H, Abu E, Moustafa H, Khodary M (1988) *J Indian Chem Soc*, 65: 827.
19. Das A, Mukhopadhayay S (2004) *Trans Metal Chem*, 29: 797.
20. Luyr'e YuYu (1967) *Spravochnik Po Analiticheskoi Khimii (Analytical Chemistry Handbook)*. Khimiya, Moscow: 248 p. (in Russian).
21. Feng W, Deng N, Glebov EM, Pozdnyakov IP, Grivin VP, Plyusnin VF, Bazhin NM (2007) *Russian Chem Bull,* International Edition, 56: 900.
22. Lur'e YuYu (1979) *Spravochnik po analiticheskoi khimii (Handbook on Analytic Chemistry)*. Khimiya, Moscow: 344 p. (in Russian).
23. Wang J, Tateno T, Sakuragi H, Tokumaru K (1995) *J Photochem Photobiol A: Chem*, 92: 53.
24. Pozdnyakov IP, Plyusnin VF, Grivin VP, Vorobyev DYu, Bazhin NM, Pagйs S, Vauthey E (2006) *J Photochem Photobiolog A: Chem*, 182: 75.
25. Pozdnyakov IP, Plyusnin VF, Tkachenko N, Lemmetyinen H (2007) *Chem Phys Lett*, 445: 203.
26. Ogawa K, Tobe N (1966) *Bull Chem Soc Japan*, 39: 223–227.
27. Son DH, Kambhampati P, Kee TW, Barbara PF (2002) *J Phys Chem A*, 106, 4591.
28. Pozdnyakov IP, Kel OV, Plyusnin VF, Grivin VP, Bazhin NM (2008) *J Phys Chem A*, 112: 8316.

29. Zuo Y, Zhan J (2005) *Atm Environ*, 39: 27.
30. Calvert J, Pitts J (1967) *Photochemistry.*Wiley, New York-London-Sydney.
31. Balzani V, Carassiti V (1970) *Photochemistry of Coordination Compounds*. Academic Press, London-New York.
32. Parker CA, Hatchard CG (1955) *Nature*, 176: 122.
33. Nadtochenko V, Kiwi J (1996) *J Photochem Photoboil A: Chem*, 99: 145.
34. Patterson JIH, Perone SP (1973) *J Phys Chem*, 77: 2437.
35. Cooper GD, DeGraff BA (1971) *J Phys Chem*, 75: 2897.
36. Chen J, Zhang H, Tomov IV, Wolfsberg M, Ding X, Rentzepis PM (2007) *J Phys Chem A*, 111: 9326.